THE PULSATION THEORY OF MIRA CETI

BY

JACOB GABOVITŠ

TARTU 1936

Printed by K. Mattiesen Ltd., Tartu, 1936.

Summary.

The following conclusions may be drawn from the results obtained.

1. On account of the great absorption in the visual region of the *M*-type variables, produced by the *TiO* atmosphere, the visual magnitude cannot be used directly to calculate the effective temperature; a good approximation to the true effective temperature of these stars may be got from the difference — photographic magnitude *minus* bolometric magnitude. The "photo-bolometric" temperature of Mira obtained in this manner (Table II) varies from 2630° (just before the maximum light) to 1690° (at the minimum light), the amplitude of variation, 940 degrees, being much greater than any other obtained before. The comparison of our "photo-bolometric" temperatures with the temperatures by Pettit and Nicholson (Fig. 1) shows that the latter temperatures are systematically too high. This circumstance is explained by the influence of *TiO* absorption on the "water-cell absorption" from which the temperatures by Pettit and Nicholson are determined.

2. From the "photo-bolometric" temperatures "ideal" colour indices are calculated which range from 2.35 to 4.19 as compared (Fig. 2) with the observed colour variation from 0.87 to 2.25 (the extreme values of the "ideal" colour index, and the observed colour index not coinciding in phase). From the difference of the "ideal" colour, and the observed colour the variation of the *TiO* colour correction is obtained (Fig. 3). The latter permits us to correct the observed visual magnitude for the *TiO* absorption which gives the "ideal" visual magnitude. The "ideal" visual magnitude varies from 2.42 to 6.95 as compared with the range of the observed visual magnitude (corrected for the visual companion) from 3.32 to 9.90. All these results are collected in Table III.

3. The angular diameter of Mira, computed from the "photo-bolometric" temperature and the "ideal" visual magnitude, varies

from 0".034 to 0".062, being greater at minimum than at maximum brightness. With an adopted parallax of Mira equal to 0".019, the corresponding values of the linear photospheric radius are 191 and 352 of the sun's radius respectively. The density of Mira, with an assumed mass of 9.6 ⊙, ranges from $13.8 \cdot 10^{-7}$ ⊙ to $2.2 \cdot 10^{-7}$ ⊙ (Fig. 5). The "photospheric" radial velocity, computed from the variation of the diameter, has a range of 32.5 km/sec, as compared with the range of 11.8 km/sec obtained by Joy from absorption lines. The dissimilarity of the two radial velocity curves (Fig. 6) is enormous, our "photospheric" radial velocity curve showing a quite peculiar and irregular trend. The difference between the recess and the approach semiamplitudes of our curve, the corresponding values being +20.4 and −12.1 km/sec respectively, is especially remarkable. The results summarized here are represented in Table IV.

4. The range of the "ideal" visual magnitude of Mira, 4.53, requires a ratio of the radii of 1.84, the radius at minimum brightness being greater. This result is confirmed by the consideration of the bolometric magnitude range obtained by Pettit and Nicholson, 0.87 mag., which gives a ratio of 1.62 of the radii in satisfactory agreement with the former value and requiring also a greater radius at minimum light. *This circumstance is certainly the most weighty argument in favour of the pulsation theory of Mira.*

5. A comparison is made of the computed angular diameter of Mira with the interferometer results obtained by Pease at two different maxima. The agreement is quite satisfactory, the difference $d''_{interf.} - d''_{comp.}$ being within the limits of the interferometer measurement error.

6. The relative temperature and radius ranges of Mira are nearly equal, their equality being required also by Eddington's pulsation theory.

7. The density variation curve of Mira resembles that expected for a pulsating star, the variation of density being great only near the maximum light, whereas during 0.6 of the whole period the density is almost constant. The logarithmic mean of the computed densities shows a satisfactory agreement with Eddington's theoretical average density of a pulsating star with the period of 332 days.

8. The "photospheric" radial velocity curve of Mira differs considerably from the radial velocity curves obtained for the Cepheids; however, the most characteristic feature of the latter, the coincidence of maximum velocity of approach with maximum light, appears also in the Mira curve. The different radial velocity curves shown by the photosphere, the absorption lines, and the emission lines can be explained with the aid of the pulsation theory as follows: the absorption line velocities occur at the chromosphere (*i. e.,* at a higher level than the photosphere); the emission line velocities represent variations of a still higher level. A considerable displacement of phase between the three radial velocity curves must be expected from the standpoint of the pulsation theory on account of the great extent of the atmosphere of Mira. The semiamplitudes of the photospheric and chromospheric radii variations are 80 and 37 radii of the sun respectively. Table V shows the change of the chromospheric radius relative to the photospheric radius.

9. From the *luminosity — radius* curve of Mira (Fig. 7), supported by Getting's corresponding curves of the Cepheids and of RV Tauri variables, we draw the following important conclusion: all regular physical variables have *bolometric magnitude — photospheric radius* curves with the same characteristic features — the curves are closed with an anti-clockwise direction of description.

10. With the increasing brightness of Mira the temperature is higher than with the equal decreasing brightness (Fig. 8). This result is confirmed by Pettit and Nicholson for five other long-period variables and by Reesinck for δ Cephei.

11. With the decreasing temperature of Mira the density is smaller than with the equal increasing temperature (Fig. 9). Reesinck's result on δ Cephei: "With decreasing temperature the ionisation is stronger than with equal increasing temperature", may be regarded as identical with our result on Mira Ceti, taking into account that stronger ionisation occurs at a smaller density.

12. With the increasing spectrum of Mira the *TiO* correction is greater than with the equal decreasing spectrum (Fig. 10). The double-valued form of the *spectrum — TiO correction* curve may be explained only on the assumption of the variable pressure possible only in case of the pulsation theory; generally, both

the spectrum and the *TiO* correction depend not only upon the quantity of *TiO* present in the star but also upon the pressure variation; a deviation from strict parallelity between the two pressure effects, together with the assumption of variable pressure, may account for the phenomenon.

13. The variation of the surface gravity of Mira (Fig. 11) is found to be similar to that obtained by Kipper for two Cepheids, the maximum of surface gravity in all three cases taking place almost exactly at the same phase (from —0.05 to —0.1). This phase, 0.90, or 0.95, apparently represents the most characteristic moment in the cyclic variation of the regular variable stars.

14. *All physical regular variables form one group of stars with the same cause of variation, pulsation being the most probable explanation of the observed phenomena.*

I. The Results.

1. Introduction.

The most serious obstacle in the study of the physical conditions of the *M*-type long-period variables is the appearance of a variable titanium oxyde atmosphere in these low temperature stars which considerably affects their visual magnitude and colour. As shown by the writer[1], the deviation from the black body radiation of the *M*-type stars is almost entirely due to *TiO* absorption.

Thus, estimating, for instance, such an important feature as the effective temperature, we must start from observational data which are not, or are only little influenced by *TiO* absorption. Such data are the radiometric and photographic magnitudes, since the *TiO* absorption is distributed mainly over the visual wave-lengths.

The difference between the photographic and bolometric magnitudes (the latter being derived from the radiometric magnitudes) gives us the true effective temperature. Further, using any colour — temperature relation, we get the "ideal" colour index, whereas the difference "ideal" colour *minus* observed colour gives us the *TiO* correction expressed in magnitudes. Finally, correcting the observed visual magnitude for the *TiO* correction found, we obtain the "ideal" visual magnitude, *i. e.* the magnitude of a star with the same true temperature distribution but without the titanium oxyde atmosphere.

Such a way of deriving the *TiO* absorption quantitatively was first used by Öpik and the writer in a paper on The Densities of Visual Binary Stars[2].

The object of the present paper is to show that by using the above described method we may obtain a reliable idea of

---

[1] J. Gabovitš, *Publ. Tartu Obs.*, **28.**5, 1936.

[2] J. Gabovitš and E. Öpik, *Publ. Tartu Obs.*, **28.**3, 1935.

the physical variations occurring in the long-period variable stars. For this purpose we chose the representative long-period variable Mira Ceti on account of the photographic and radiometric light curves available for it.

2. The Observational Data.

In Table I are collected the observational data for Mira Ceti. The subsequent columns give:

1. The visual phase; the phases considered are not equidistant, on account of the slow variation taking place on the descending branch and the much greater variation on the ascending one.

2. and 3. The observed photographic and the visual apparent magnitudes derived from the corresponding light curves, published by Miss Cannon[3].

4. The colour index *(C)*, from the data in columns 2 and 3. It must be remarked that the colour of Mira at minimum light, 1.24 mag., is possibly slightly underestimated on account of the influence of the *B* class[4] visual companion. However, the fact that in all known cases the colour indices of the long-period variables at minimum lie near 1.0 mag.[5] seems to indicate that the above quoted value of the colour of Mira at minimum is not far from the truth.

5. and 6. The photographic (m_p) and visual (m_v) magnitudes, corrected for the light of the companion. The magnitude of the companion was assumed to be 9.8, according to Aitken[6].

7. The radiometric (m_r) magnitude, as given by Pettit and Nicholson[7].

8. The atmospheric absorption of the radiometric magnitude, Δm_r (a function of the temperature[8]); Δm_r was determined by successive approximations.

---

[3] Annie J. Cannon, *Harv. Bull.*, **872,** 28, 1930.

[4] A. H. Joy, *Mt. Wilson Contr.*, No. **311,** 1926, page 54.

[5] B. P. Gerasimovič and H. Shapley, *Harv. Bull.*, **872,** 25, 1930.

[6] R. G. Aitken, *Publ. A. S. P.*, **35,** 323, 1923.

[7] E. Pettit and S. B. Nicholson, *Mt. Wilson Contr.*, No. **478,** 1933, page 17.

[8] *Ibid.*, page 15.

9. The bolometric (m_b) magnitude, derived from Pettit and Nicholson's formula[9]

$$m_b = m_r - \Delta m_r + 0.9 \quad . \quad . \quad . \quad (1).$$

10. The spectrum, according to Joy's spectrum — visual magnitude relation (*cf.*[4], Table III).

Table I.

Observational data for Mira Ceti.

1	2	3	4	5	6	7	8	9	10
	combined			corr. for comp.					
V. Ph.	m_p	m_v	C	m_p	m_v	m_r	Δm_r	m_b	Sp.
	m	m	m	m	m	m	m	m	
0.00	4.81	3.32	1.49	4.81	3.32	— 0.19	0.54	0.17	*M* 5.6
.05	5.17	3.41	1.76	5.17	3.41			.10	5.8
.10	5.49	3.74	1.75	5.50	3.75	— 0.28	.59	.03	6.3
.20	6.39	5.13	1.26	6.41	5.15	— 0.21	.65	.04	7.3
.30	7.38	6.51	0 87	7.43	6.56	— 0.01	.69	.20	8.0
.40	8.50	7.61	0.89	8.65	7.76	+ 0.31	.74	.47	8.4
.50	9.62	8.48	1.14	10.00	8.86	+ 0.58	.80	.68	8.8
.60	10.26	9.05	1.21	11.01	9.80	+ 0.83	.84	.89	9.1
.65	10.34	9.10	1.24	11.14	9.90			.90	9.1
.70	10.24	8.93	1.31	10.89	9.58	+ 0.83	.83	.90	9.0
.75	9.93	8.52	1.41	10.32	8.91			.85	8.8
.80	9.46	7.82	1.64	9.65	8.01	+ 0.68	.77	.81	8.5
.85	8.00	6.27	1.73	8.04	6.31			.72	7.9
.90	6.00	3.81	2.25	6.07	3.82	+ 0.33	0.60	.63	6.4
0.95	4.90	3.43	1.47	4.90	3.43			0.40	*M* 5.8

3. The Temperature.

Using the data in columns 5 and 9 of Table I we may obtain the true effective temperature (T) of Mira throughout all phases according to the formula (*cf.*[2]):

$$m_p - m_b = \frac{36100}{T} + 10 \log T - 43.40 \quad . \quad . \quad . \quad (2).$$

Table II, column 3, shows the computed temperatures. The minimum value of our "photo-bolometric" temperature, 1690° K, coincides with the minimum light of Mira, whereas the maximum temperature, 2630° K, is reached at the visual phase 0.95.

In Table II and Fig. 1 the "photo-bolometric" temperatures are compared with the "water-cell" temperatures (T_{wc}) obtained

[9] *Ibid.*, page 11.

by Pettit and Nicholson[10]. The values of T_{wc} are systematically too high, the difference $T_{wc} - T$, as given in column 5 of Table II, increasing toward the minimum light. This seems to indicate

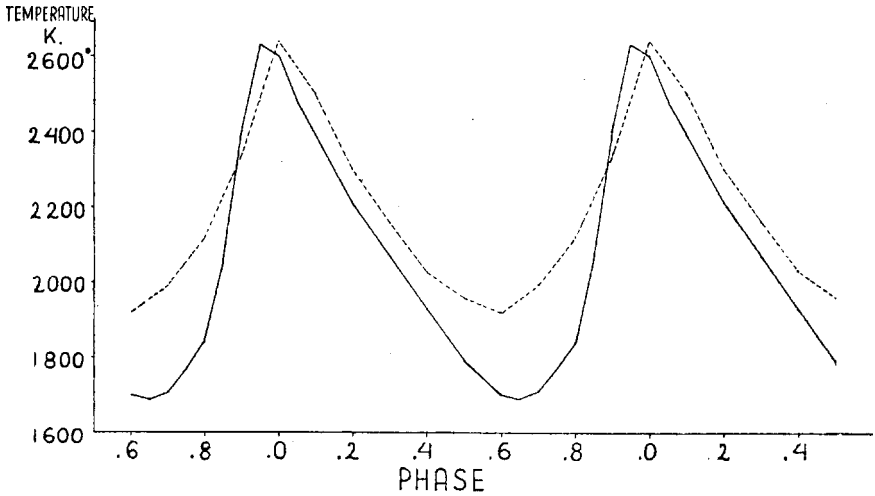

Fig. 1. Variation of temperature of Mira. Full line — true effective temperature; broken line — "water-cell" temperature.

that the influence of *TiO* absorption on the "water-cell absorption", suggested by Pettit and Nicholson[11], increases with the decreasing light of the star.

Table II.

True Effective Temperature *(T)* of Mira.

1 V. Ph.	2 $m_p - m_b$	3 T	4 T_{wc}	5 $T_{wc} - T$	1 V. Ph.	2 $m_p - m_b$	3 T	4 T_{wc}	5 $T_{wc} - T$
	m					*m*			
0.00	4.64	2600°	2640°	40°	0.65	10.24	1690°		
.05	5.07	2480			.70	9.99	1710	1990°	280°
.10	5.47	2390	2500	110	.75	9.47	1770		
.20	6.37	2210	2300	90	.80	8.84	1840	2120	280
.30	7.23	2070	2160	90	.85	7.32	2050		
.40	8.18	1930	2030	100	.90	5.44	2400	2340	—60
.50	9.32	1790	1960	170	0.95	4.50	2630		
0.60	10.12	1700	1920	220					

[10] *Ibid.*, page 17.
[11] *Ibid.*, page 14.

4. The "Ideal" Colour and the "Ideal" Magnitude.

For the colour-temperature relation we use the well-known expression with Öpik's constants[12] reduced[13] to the Harvard colour system:

$$\frac{C_2}{T} = 1.65\,C' + 1.56 \quad . \quad . \quad . \quad (3),$$

where C' is the "ideal" colour index, and $C_2 = 14300$.

After calculating the "ideal" colour indices from the temperatures given in column 3 of Table II, we obtain the *TiO* correction *(ΔC)* from

$$\Delta C = C' - C \quad . \quad . \quad . \quad (4),$$

where the observed colour C is taken from Table I, column 4. The "ideal" apparent visual magnitude (m'_v) is given then by

$$m'_v = m_v - \Delta C \quad . \quad . \quad . \quad (5),$$

where m_v is got from column 6 of Table I.

Table III contains the results of the computation. *Column 2* shows the "ideal" colour indices computed from formula (3). The "ideal" colour varies from 2.35 to 4.19, the range being thus 1.84 mag. In Fig. 2 the "ideal" colour variation curve (the upper curve) is compared with the observed one (the lower

Table III.

"Ideal" Colour *(C')*, *TiO* Correction *(ΔC)*, and "Ideal" Magnitude (m'_v).

1 V. Ph.	2 C'	3 ΔC	4 m'_v	1 V. Ph.	2 C'	3 ΔC	4 m'_v
	m	m	m		m	m	m
0.00	2.39	0.90	2.42	0.65	4 19	2.95	6.95
.05	2.55	0.79	2.62	.70	4.12	2.81	6.77
.10	2.68	0.93	2.82	.75	3.95	2.54	6.37
.20	2.98	1.72	3.43	.80	3.76	2.12	5.89
.30	3.24	2.37	4.19	.85	3.28	1.55	4.76
.40	3.55	2.66	5.10	.90	2.67	0.42	3.40
.50	3.90	2.76	6.10	0.95	2.35	0.88	2.55
0.60	4.15	2.94	6.86				

[12] E. Öpik, *Ap. J.*, **81**, 177, 1935.

[13] E. Öpik, *Publ. Tartu Obs.*, **27**.1, Table I, 1929.

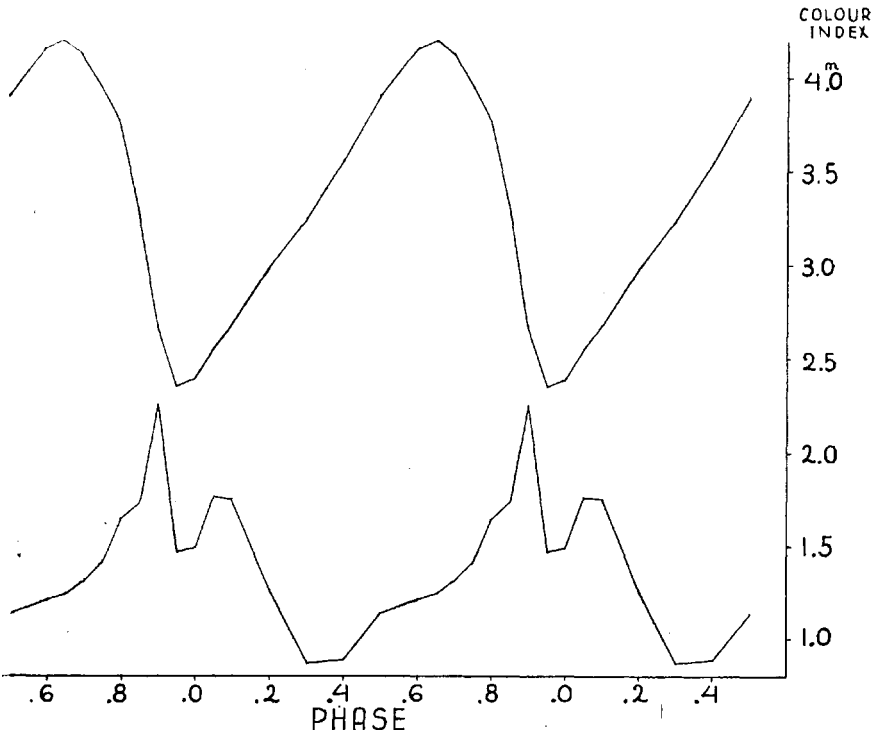

Fig. 2. Comparison of "ideal" colour (upper curve) with observed colour (lower curve) of Mira.

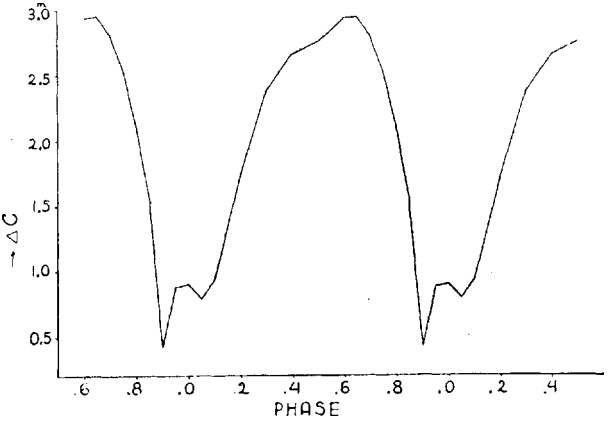

Fig. 3. Variation of *TiO* colour correction (ΔC) of Mira.

curve). It is remarkable that the jumps and inequalities present in the latter curve fail to appear in the "ideal" colour curve. *Column 3* contains the *TiO* correction ΔC, defined by (4). This correction reaches its maximum value, 2.95 mag., at the minimum light of Mira, while the minimum value of the *TiO* correction, 0.42 mag., falls into the visual phase 0.90. This result shows the interesting fact that the smallest quantity of *TiO* in the star does not appear at the maximum light but slightly before it.

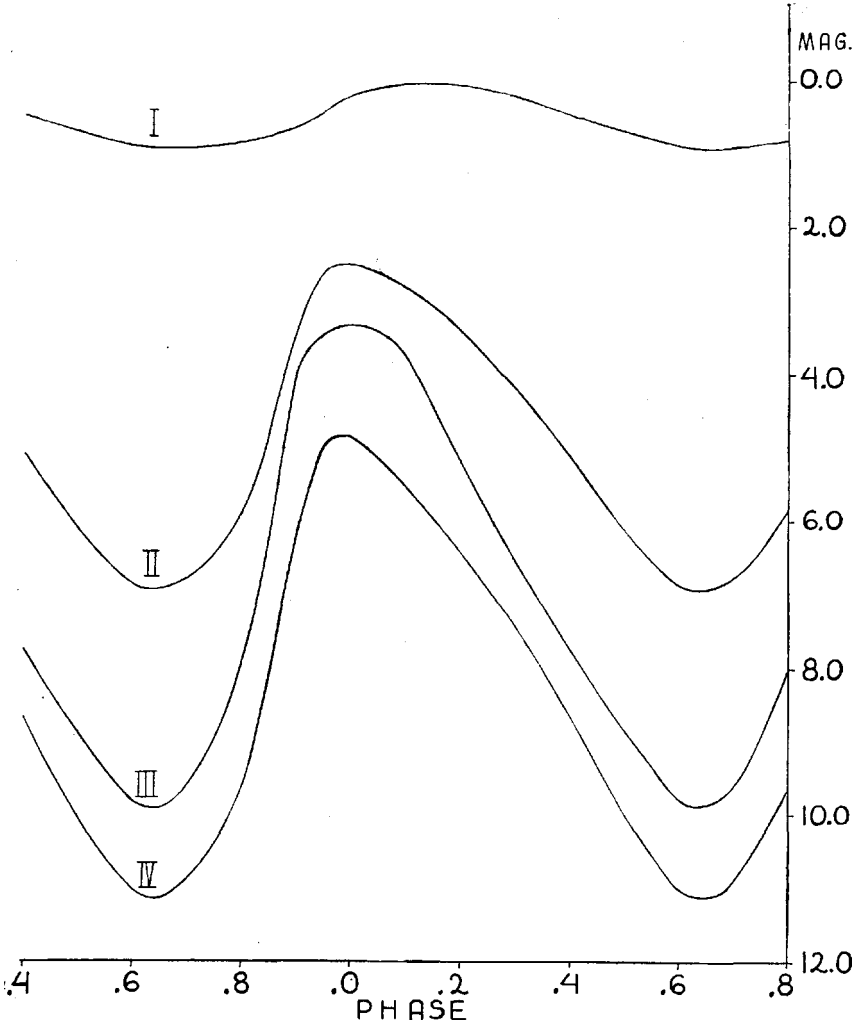

Fig. 4. Bolometric (I), "ideal" visual (II), observed visual (III), and photographic (IV) light curves of Mira.

Fig. 3 shows the ΔC variation curve graphically. *Column 4* gives the "ideal" apparent visual magnitudes m'_v, defined by (5).

In Fig. 4 the "ideal" visual light curve (II) is compared with the observed visual (III), the photographic (IV), and the bolometric (I) light curves. It is remarkable that the visual light curve corrected for the *TiO* absorption assumes a different form as compared with the uncorrected curve becoming now more similar to the photographic light curve.

5. The Diameter, Density, and "Photospheric" Radial Velocity.

The subsequent columns of Table IV contain:

1. The visual phase;
2. The angular diameter *(d'')*, computed from

$$\log d'' = \frac{5400}{T} - 0.2m'_v - 3.016 \quad . \quad . \quad . \quad (6),$$

where $\lambda_{max.} = 0.575$ is assumed for the effective visual wavelength of the *M*-type variables[14].

3. The linear radius R (sun = 1), derived from the data in column (2), and from the parallax of Mira. The latter we assume to be 0''.019 according to the apparent visual magnitude at maximum used in this paper and an absolute visual magnitude —0.3, estimated by Joy[15].

4. The density ϱ (sun = 1). The mass of Mira was assumed to be 9.6 ⊙ according to the mean bolometric absolute magnitude —3.14 and the empirical mass — luminosity relation by Kopal[16]. The density variation curve is given by Fig. 5.

5. The "photospheric" radial velocity corrected for the average projection on the line of sight, obtained from the smoothed radius variation curve. In Fig. 6 our "photospheric" radial velocity curve (full line) is compared with the radial velocity curve obtained by Joy from absorption lines[17]. The dissimilarity of both curves is enormous. Contrary to the "ordinary" and smooth trend of Joy's curve, our radial velocity curve shows a quite peculiar nature, also having a much greater range of 32.5 km/sec, as compared with the 11.8 km/sec of the radial velocity range by Joy.

[14] A. H. Joy, *loc. cit.*, page 50.
[15] *Ibid.*, page 49.
[16] Z. Kopal, *Zs. f. Ap.*, **9**, 239, 1935.
[17] *Loc. cit.*, page 18.

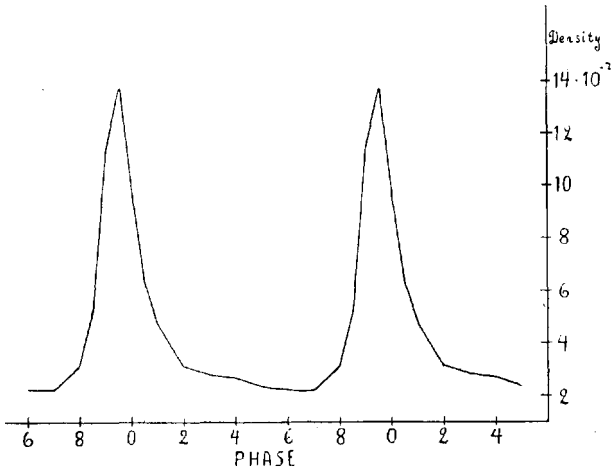

Fig. 5. Density variation curve of Mira.

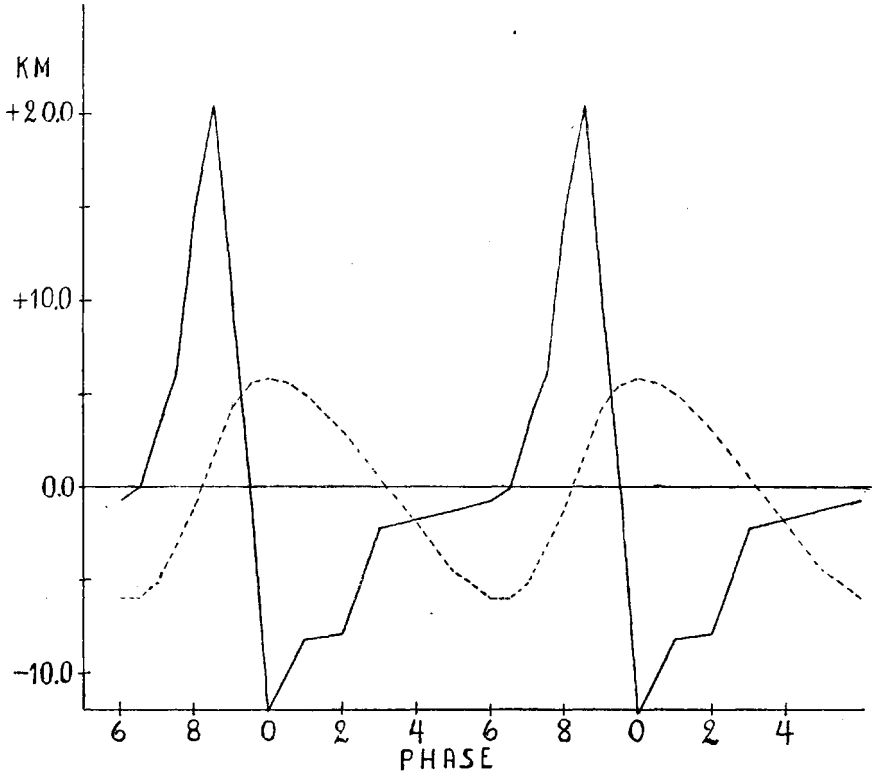

Fig. 6. Variation of "photospheric" (full line) and "chromospheric" (broken line) radial velocities of Mira.

Table IV.

Angular Diameter *(d'')*, Linear Radius *(R)*, Density *(ϱ)*, and "Photospheric" Radial Velocity *(v)*.

1 V. Ph.	2 d''	3 R	4 ϱ	5 v	1 V. Ph.	2 d''	3 R	4 ϱ	5 v
0.00	0″.038	215	$9.66 \cdot 10^{-7}$	—12.1	0.65	0″.062	352	$2.22 \cdot 10^{-7}$	0.0
.05	.043	247	6.38	—10.1	.70	.061	349	2.26	+ 3.3
.10	.048	272	4.78	— 8.2	.75	.058	329	2.71	+ 6.0
.20	.055	313	3.13	— 7.9	.80	.055	313	3.16	+15.0
.30	.057	323	2.86	— 2.2	.85	.046	264	5.26	+20.4
.40	.058	329	2.71	— 1.7	.90	.036	204	11.40	+ 9.9
.50	.060	344	2.38	— 1.2	0.95	0″.034	191	$13.76 \cdot 10^{-7}$	0.0
0.60	0″.061	349	$2.26 \cdot 10^{-7}$	— 0.7					

II. Discussion.

6. The Long-Period and Cepheid Variables.

Several astronomers have pointed out the possible similarity in many physical properties between the long-period variables and the Cepheids. This led them to the suggestion that both classes of variables form a natural sequence of stars with the same cause of variation. Some investigators confine themselves to that conclusion, considering the Cepheids and the Mira stars as one group of variables, without specifying the possible cause of their light variation. Joy says in his Spectrographic Study of Mira Ceti[18]: ". . . the physical changes may be traced to sources similar to those prevailing in the hotter variable stars and . . . the whole group of physical variables may be found to form a sequence from the shortest to the longest periods."

However, some astronomers who consider both classes of variables together come to the definite conclusion that the most probable explanation of the largest number of observations is a periodic pulsation of these stars. Eddington says[19]: "There is growing evidence that long-period variation and Cepheid variation are essentially the same phenomenon. The very low density and temperature of the long-period variables exaggerates and renders

[18] *Loc. cit.*, page 60.

[19] A. S. Eddington, The Internal Constitution of the Stars, Cambridge, 1926, page 206.

more erratic the effects of the same kind of pulsation as in the Cepheids." While Eddington's conclusion is "still very speculative"[20], Shapley makes the same deduction by the aid of pure observational results[21]: "it appears that the pulsation hypothesis can be logically extended to long-period variation on the basis of the observed similarity with Cepheids in bolometric absolute magnitude, radiation variations, spectral peculiarities, and galactic distribution". The recently published theoretical investigation on the constitution of the stars by Anderson[22] occupies a quite isolated place in the question considered. He points out *the aptitude of the red giants to pulsate caused by a small spontaneous variation in bolometric magnitude.* He writes[23]: „Es ist zu beachten, daß bei den oberen Gliedern der *g*-Reihe (mit niedriger effektiver Temperatur) die geringste Variation der absoluten bolometrischen Helligkeit eine bedeutende Expansion (oder Kontraktion) des Sterns hervorrufen muss. Daraus folgt, daß rote Riesen wenig stabil und zum Pulsieren geneigt sein müssen." Anderson's conclusion is of very great importance because of its complete independence of the Cepheid variables. Since, historically, pulsation was first suspected in the Cepheids, and only the similarity of the Mira stars led to the extension of the pulsation theory over the long-period variables, Anderson's results seem to indicate that it is more natural that pulsation may be supposed to exist just in the long-period variable stars, and thus the train of ideas must be inverted.

7. The Range of the "Ideal" Visual Magnitude.

The "ideal" visual magnitudes (cf. Section 4, Table III) at maximum and minimum light are 2.42 and 6.95, as compared with the observed corresponding values 3.32 and 9.90. Thus, the range of the "ideal" visual magnitude is 4.53. Theoretically the range of the visual magnitude may be computed from

$$m_{min.} - m_{max.} = \frac{27000}{T_{min.}} - \frac{27000}{T_{max.}} + 5 \log \frac{R_{max.}}{R_{min.}} \quad . \quad . \quad . \quad (7),$$

where T, and R denote the temperature and the radius respec-

[20] *Ibid.*

[21] H. Shapley, *Harv. Bull.*, **861**, 1, 1928.

[22] W. Anderson, *Publ. Tartu Obs.*, **29.1**, 1936.

[23] *Ibid.*, page 118.

tively, and the indices *max.* and *min.* refer to the maximum and minimum light; $\lambda_{(max.)} = 0.575$ is assumed according to Joy (*cf.* Section 5).

If we assume a constant radius, the amplitude of the "photobolometric" temperature variation (*cf.* Section 3, Table II) requires a range of the visual magnitude equal to 5.58 mag., whereas the range of the "ideal" magnitude is only 4.53. Thus, *the assumption of a variable radius (namely, a greater radius at minimum light than at maximum) leads to a better agreement with the range of the "ideal" visual magnitude than the assumption of a constant radius.*

This important result is confirmed by the consideration of the bolometric magnitude range for which we have the formula

$$m_{min.} - m_{max.} = 10 \log \frac{T_{max.}}{T_{min.}} + 5 \log \frac{R_{max.}}{R_{min.}} \quad . \quad . \quad . \quad (8).$$

Supposing the radius to be constant, we get the bolometric range 1.92 mag., whereas the observed range of the bolometric magnitude is only 0.87 (*cf.* Section 2, Table I) requiring the radii ratio $\frac{R_{min.}}{R_{max.}} = 1.62$ in satisfactory agreement with the value found from the visual magnitude range, 1.84. Thus, *the range of the bolometric magnitude suggests also a variable radius and a smaller radius at maximum light.*

8. Comparison of the Computed Diameter with Interferometer Data.

An interesting comparison of the calculated angular diameter at maximum light may be made with the interferometer results obtained by Pease at two different maxima. The first measurement, which gave the value 0".056[24], was made at the January 1925 maximum when the star reached the magnitude 3.8 only[25], whereas the second result, $d'' = 0''.047$[26], was got at the 1928 maximum when the magnitude of Mira was 3.1[27].

If we assume that the physical conditions of Mira at the 1925 maximum correspond to those at a normal visual phase of

[24] F. Pease, *Publ., A. S. P.*, **37,** 90, 1925.
[25] A. H. Joy, *loc. cit.*, page 8.
[26] F. Pease, *Publ. A. S. P.*, **41,** 333, 1929.
[27] F. Lause, *Beob.-Zirk. der A. N.*, nr. 1. 1929.

0.1, while the maximum of 1928 may be regarded as a normal maximum, our computed angular diameters are correspondingly 0″.048 and 0″.038 (*cf.* Section 5, Table IV). The agreement is quite satisfactory, the differences $d''_{interf.} - d''_{comp.}$ being 0″.008 and 0″.009 only within the limits of the interferometer measurement error.

As shown by the data in column 2 of Table 4, the computed diameter decreases with increasing magnitude. The fact, that the measured diameter shows the same tendency, leads us to the conclusion that possibly *the different results obtained by the two interferometer measurements are due not to observational errors but to a real variation of the diameter.*

9. The Radius and Temperature Variation.

The range of the photospheric radius of Mira (*cf.* Section 5, Table IV) is very great, 161 sun's radii, being much greater than the corresponding value for the Cepheids. The obtained radius range of Mira is possibly slightly overestimated, on account of the uncertainty of the minimum temperature and the visual brightness data, but there is no doubt that the order of magnitude of the range is correct in accordance with Anderson's theoretical suggestion[28].

The relative temperature and radius ranges of Mira, $\frac{\delta T}{T_m}$ and $\frac{\delta R}{R_m}$, where δT and δR denote the semiamplitudes of the variation of T and R, while T_m and R_m are the mean temperature and radius, are 0.22 and 0.28 respectively. Both values are approximately equal, their equality being required also by Eddington's pulsation theory. For a number of Cepheids Eddington finds the corresponding values to be 0.066 and 0.073[29].

10. The Density.

Fig. 5 shows the density variation of Mira, the curve obtained resembling that expected for a pulsating star. The greatest density (and the smallest radius) occurs slightly before the maximum ghlit, at the phase 0.95, where it begins rapidly to diminish; between the phases 0.2 and 0.8 (*i. e.* during 0.6 of the whole

[28] *Loc. cit.*, page 118.

[29] *Loc. cit.*, page 185.

period) the variation of density is very small, and from the phase 0.8 on it increases again with great rapidity.

As to the theoretical period — density relation, Eddington's equation[30]

$$P\sqrt{\varrho_c} = 0.290\ (\gamma a)^{-\frac{1}{2}} \quad . \quad . \quad . \quad (9),$$

where P is the period, ϱ_c the central density, γ the effective ratio of specific heats, and $\gamma a = 3\gamma - 4$, permits us to calculate the expected average density of a pulsating star with a period of 332 days. We assume: $\varrho_c = 54\,\varrho_m$, $(\gamma a)^{\frac{1}{2}} = 0.3$. Equation (9) gives then $\varrho_m = 1.6 \cdot 10^{-7}$, in satisfactory agreement with the logarithmic mean value of our computed densities, $4.0 \cdot 10^{-7}$.

11. The Radial Velocities.

The "photospheric" radial velocity curve, shown by Fig. 6 (full line), seems to represent, like the above considered density curve (Fig. 5), the peculiar behaviour of an oscillating star. The maximum velocity of recess occurs at the phase 0.85, 0.1 of the period before the smallest radius, whereas already at the maximum light the maximum velocity of approach is reached.

Although the general trend of the curve considered differs considerably from the radial velocity curves obtained for the Cepheid variables, it is noteworthy that the most characteristic feature of the latter, namely the coincidence of maximum velocity of approach with maximum light, appears also in the Mira curve. A further interesting feature of our "photospheric" velocity curve is the different values of the maximum velocities of recess and approach; while the former value is 20.4 km sec, the greatest velocity of approach is 12.1 km/sec only. If this phenomenon is real, it may play an important rôle in further studies on the causes of pulsation.

Considering the radial velocity curve obtained by Joy from absorption lines[31] (Fig. 6, broken line), its behaviour and dissimilarity with the "photospheric" radial velocity curve seems at the first glance to present no explanation. However, the pulsation theory makes it possible reliably to explain the correlation between both curves.

[30] *Ibid.*, page 192.

[31] *Loc. cit.*, page 18.

The velocities given by the absorption lines evidently occur at a higher level than the photosphere, namely at the reversing layer (lower chromosphere). Thus, contrary to the "photospheric" radial velocities computed in this paper, we may call the absorption line velocities the "chromospheric" radial velocities; they represent the variation of the chromospheric radius. On account of the doubtlessly large chromosphere of Mira a great displacement of phase between the "photospheric" and the "chromospheric" velocity curves is to be expected. It is also very probable that the irregular variation of the photospheric radius is not translated upon the chromospheric radius, the variation of the latter being thus more regular. The range of the "chromospheric" velocity curve is smaller than that of the „photospheric" velocity curve as shown by Fig. 6. This circumstance requires a smaller range of the chromospheric radius. While the semiamplitude of the photospheric radius variation is 80 sun's radii (*cf.* Section 9), the corresponding value for the chromospheric radius, as found by Joy from the spectroscopic elements, is 26200000 km[32], or about 37 sun's radii.

In order to make evident the correlation between the photospheric and chromospheric radii, we give the following table, which shows clearly the change of the chromospheric radius relative to the photospheric radius.

Table V.

Variation of Photospheric and Chromospheric Radii.

Phase	Photospheric Radius	Chromosph. Radius	"Photospheric" Radial Velocity	"Chromospheric" Radial Velocity
0.00	small; increase	decrease	maximum approach	maximum recess
.32	large; increase	smallest	slight approach	zero
.65	largest	increase	zero	maximum approach
.82	large; decrease	largest	rapid recess	zero
.85	intermediate; decrease	decrease	maximum recess	slight recess
0.95	smallest	decrease	zero	rapid recess

[32] *Ibid.*, page 19.

As to the emission line velocities, determined also by Joy[33], their difference from the absorption line velocities follows inevitably from the pulsation theory. The emitting layer of the long-period variables lies still higher than the absorbing one[34], which circumstance must necessarily cause a displacement of phase between the absorption and the emission velocity curves. Unfortunately, emission line velocities are not determinable between the phases 0.6 and 0.9, the behaviour of the emission line velocity curve in this region remaining open. The extrapolation suggested by Joy is probably not well founded, because it would indicate a permanent approach of the emitting layer during the whole period, which evidently cannot be real.

12. The Luminosity — Radius Diagram.

Some years ago Milne proposed a new method of analysing stellar variability[35], consisting of a construction of the bolometric luminosity — radius diagram. Getting applied this new method to some variable stars[36], Cepheids, RV Tauri variables, and long-period variables. As to the Cepheids and RV Tauri variables, Getting finds their luminosity — *log*radius ("characteristic") curve to be in all cases a closed curve, with motion in the anti-clockwise direction.

On the basis of the data obtained in this paper, we traced the corresponding diagram for Mira Ceti (Fig. 7). The result is surprising and highly significant: *the m_b — log R curve of Mira is closed with a motion in the anti-clockwise direction, thus having the same characteristics as the Cepheid and RV Tauri variable curves.*

It is interesting to remark that Getting's own curve for Mira Ceti, contrary to our result, shows a clockwise direction of description. This disagreement is evidently explained by the fact that Getting used the absorption line velocities, which give the chromospheric radius, for deriving the radius of Mira, whereas the photospheric radius must be regarded as characteristic. Indeed, the radii used by Getting for the Cepheids are also chromospheric

[33] *Ibid.*, pages 18, 39.
[34] *Ibid.*, page 60.
[35] E. A. Milne, *M. N.*, **94,** 418, 1934.
[36] J. A. Getting, *M. N.*, **95,** 139, 1934.

radii, but there the phase displacement between the photospheric and the chromospheric radii variation is not so much appreciable as in the long-period variables.

From the results obtained Getting proposed the following method of classification of all regular variables into three classes[37]: "(1) stars which have one simple loop in their characteristic curve traced in the anti-clockwise direction; (2) stars which have one

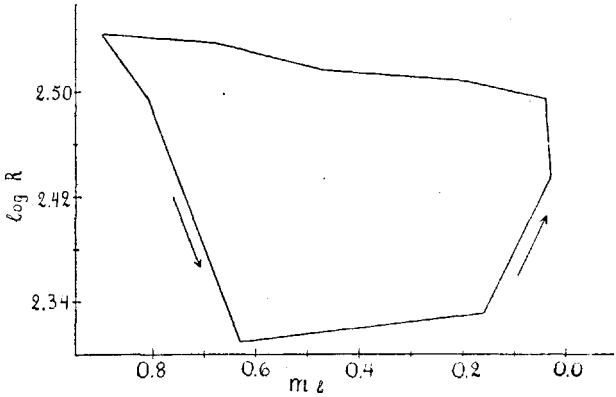

Fig. 7. Luminosity — radius diagram of Mira. Abscissae — bolometric magnitude; ordinates — logarithm of radius.

simple loop in their characteristic curve traced in the clockwise direction; and (3) stars possessing complicated characteristic curves." The corresponding classes of variables, according to Getting, are: (1) the Cepheids; (2) the long-period variables; (3) the RV Tauri variables.

With our result on Mira's "characteristic" curve (which may be expected to hold for all *M*-type variables) Getting's classification loses its reality. The erroneous opinion, that the long-period variables have "characteristic" curves with an opposite sense of description as the Cepheids, led Milne to the supposition[38] that "as we pass from the Cepheids to *M*-type variables, the characteristic curve gradually closes up to an arc enclosing zero area and then opens out again with reversed sense of description." However, Milne's supposition is not confirmed by Getting's investigation. This circumstance, as well as our result

[37] *Ibid.*, page 157.
[38] *Loc. cit.*, page 425.

on Mira's "characteristic" curve, seems to indicate that variables with a clockwise direction of their "characteristic" curves do not exist at all. This leads us to the extremely significant conclusion with respect to all considered variables: *all regular physical variable stars have bolometric luminosity — photospheric radius curves with the same characteristic features — the curves are closed with anti-clockwise direction of description.* This conclusion shows the close relationship of all three classes of the variables considered.

13. The Luminosity — Temperature and Temperature — Density Diagrams.

In a study of the spectrum of δ Cephei Reesinck[39] gets the following results: "(1) with increasing brightness the tempera-

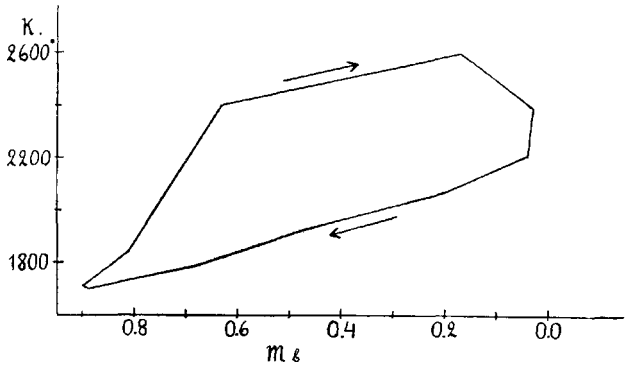

Fig. 8. Luminosity — temperature diagram of Mira.

ture is higher than with equal decreasing brightness; (2) with decreasing temperature the ionisation is stronger than with equal but increasing temperature."

On Fig. 8 we plotted the bolometric magnitudes against the "photo-bolometric" temperatures computed in this paper. As shown by the curve obtained, we get for Mira Ceti the same result as was found by Reesinck for δ Cephei: *with the increasing brightness of Mira the temperature is higher than with the equal decreasing brightness.* Our result for Mira Ceti is confirmed also by Pettit and Nicholson[40], who used their "water-cell absorption"

[39] J. Reesinck, *B. A. N.*, **4**, 41, 1927.

[40] *Loc. cit.*, page 12.

temperatures; they found the same phenomenon still for five other long-period variables.

As to Reesinck's second conclusion on δ Cephei, it may evidently be formulated in another manner, taking into account the fact that the ionisation is stronger at smaller density: with decreasing temperature the density is smaller than with equal but increasing temperature. As shown by Fig. 9, where the

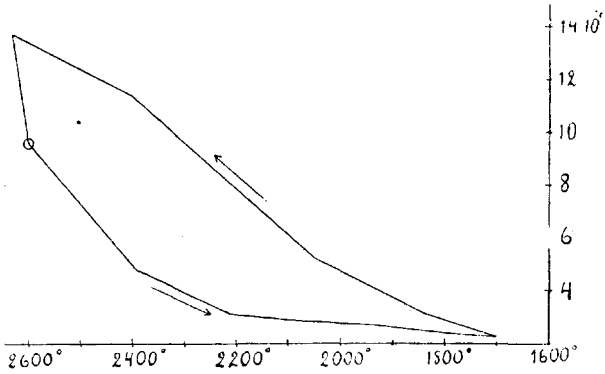

Fig. 9. Temperature — density diagram of Mira.

"photo-bolometric" temperatures are plotted against the computed densities (*cf.* Section 5, Table 4), *the same phenomenon persists also in Mira Ceti.* This fact seems to be fair evidence for the reliability of the pulsation theory.

14. The Spectrum — *TiO* Correction Diagram.

Plotting the *TiO* correction (*cf.* Section 4) against the spectrum of Mira (Fig. 10) we arrive at the interesting result that *with an increasing spectrum the TiO correction is greater than with an equal but decreasing spectrum.*

If the phenomenon obtained is real, it may be explained only on the assumption of a variable pressure, possible only in the case of the pulsation theory.

Indeed, the spectrum and the *TiO* correction are functions of the intensity of *TiO* bands, but, evidently, not exactly of the same selection of bands; on the other hand, the intensity of bands is, among others, a function of pressure; if this function of pressure does not run exactly parallel for the two selections

of bands, a double-valued form of the spectrum — *TiO* correction correlation curve may result as actually observed.

Thus, the *M*-type variables furnish us with a new possibility, not present in the Cepheids, of proving the pulsation theory, namely the closed nature of the spectrum — *TiO* correction curve. The reality of the phenomenon found seems to be

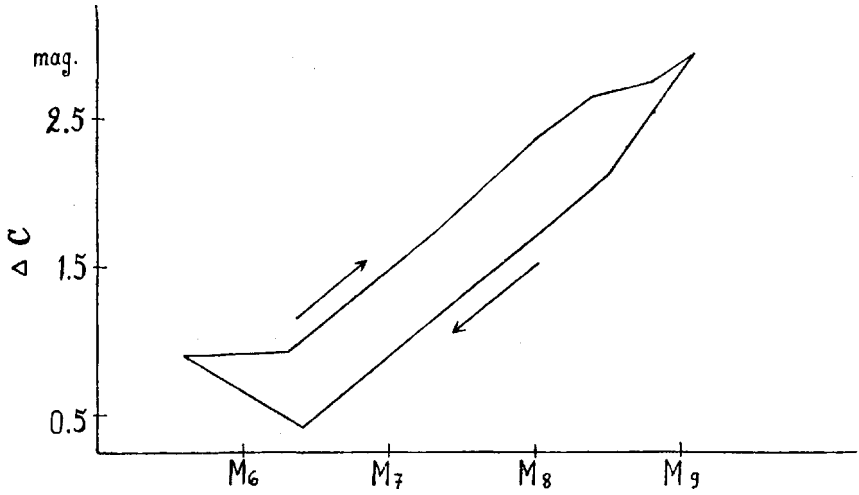

Fig. 10. Spectrum — *TiO* colour correction *(Δ C)* diagram of Mira.

evidenced by the fact that the spectrum — temperature curve of Mira forms a single arc which would not be the case if the closed form of the spectrum — *TiO* correction curve were caused by observational errors.

In concluding this section, it may be remarked that the spectrum — *TiO* correction correlation of Mira does not coincide with that of the *M* stars in general[41]. This circumstance must not be interpreted as a systematic deviation from the general "spectrum — *TiO* correction law", but is produced merely by the different systems of colour used in both determinations, since in the first case we used the Harvard colour system and in the latter the Öpik colour system.

[41] J. Gabovitš and E. Öpik, *loc. cit.*; J. Gabovitš, *loc. cit.*

15. The Surface Gravity.

In a study on the variation of surface gravity upon δ Cephei and η Aquilae, Kipper[42] reaches the following conclusion: "The surface gravity of δ Cephei and η Aquilae is constant throughout the greater part of the time. Only about 0.1 of the period before the maximum light does it grow four times as much as its general value and then falls again rapidly."

From our computed radius and the adopted mass of Mira we computed its surface gravity variation as given in Table VI.

Table VI.

Surface Gravity Variation of Mira Ceti.

Phase	log g	g	Phase	log g	g
0.00	—3.68	$2.1 \cdot 10^{-4}$	0.65	—4.11	$7.7 \cdot 10^{-5}$
.05	—3.80	1.6	.70	—4.10	7.9
.10	—3.89	1.3	.75	—4.05	8.9
.20	—4.01	$9.8 \cdot 10^{-5}$	.80	—4.01	9.8
.30	—4.04	9.2	.85	—3.85	$1.4 \cdot 10^{-4}$
.40	—4.05	8.9	.90	—3.64	2.3
.50	—4.09	8.1	0.95	—3.58	2.6
0.60	—4.10	7.9			

As shown by Fig. 11, which represents the surface gravity variation curve of Mira, Kipper's conclusion referring to the two

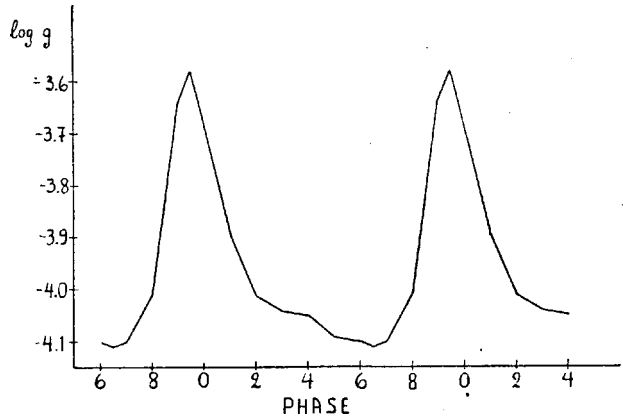

Fig. 11. Variation of surface gravity of Mira.

[42] A. Kipper, *Acta et Commentationes Univ. Tartuensis*, A, **27**, part 9, 1934.

Cepheids may be drawn also for Mira Ceti. It is especially noteworthy that the maximum surface gravity of Mira falls almost on the same phase of the period as that of the two considered Cepheids, namely 0.05 (instead of 0.1) of the period before the maximum light. The fact that also the radius, the temperature, the colour, the radial velocity, *etc.* of Mira Ceti reach their extreme values slightly before the maximum light seems to indicate that the phase 0.90, or 0.95, plays a prominent and important role in the cyclic evolution of the pulsating stars.

16. Conclusion.

As shown by the several points of the present investigation, *the results obtained furnish a decided confirmation of the pulsation theory which apparently may be extended to all long-period variables* although our conclusions are based on Mira Ceti alone. For further evidence, detailed data on bolometric magnitude, photographic magnitude and spectrum variation for other long-period variables such as are available for Mira Ceti, and which have been used here, are necessary.

I am greatly indebted to Dr. Ernst Öpik for some valuable suggestions referring to the manuscript of the present paper and to Mag. Aksel Kipper for kind information on the recent literature on the Cepheid variables.

Tartu, September 1936.